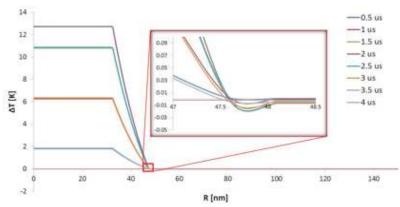## Protein coat refractive index and thermo-optical effects

A change in the refractive index n and thermo optic coefficient dn/dT of the medium surrounding a AuNP can affect the optical signal. The magnitude of these effects is discussed here.

In proteins, the index of refraction depends on their size and varies between 1.5 to 1.4 for 20kDa and 350kDa, respectively.[1] Accordingly, the refractive index of the 40kDa Gag protein (hydration neglected) can be estimated at ~1.47. The thermo-optical coefficient is not known, but can be estimated from the index of refraction and the volumetric expansion factor of proteins of $1.5\text{-}3.5\text{x}10^{-4}$ K^{-1} which results in a dn/dT of $1\text{-}2\text{x}10^{-4}$ K^{-1}, quite similar to $1\text{x}10^{-4}$ K^{-1} in water.[2] Moreover, as discussed in the manuscript the protein layer is not an infinite homogeneous layer. The protein layer in Gag-VLPs exhibits a hydration of 20-40%, a finite layer thickness of 15 nm, and pores reducing the total volume to <70% of the capsid layer. Consequently, the effective refractive index and thermo-optic coefficient are those of a protein-water mixed layer of a thickness which is comparable with the decaying length of the Au NP surface plasmon polaritons.[3]

Thus, the index of refraction of the hydrated proteins was calculated as the sum of the volumetric fraction-weighted indices of water and Gag protein. Hence, a full layer of hydrated Gag proteins exhibits an index of refraction of $n=1.44\text{-}1.41$ compared to $n=1.33$ of water. Accordingly, due to its linear dependence on the protein concentration, the dn/dT of the hydrated protein layer reduces to $1.6\text{-}1.8\text{x}10^{-4}$ K^{-1} for 40 and 20% hydration, respectively. Considering the pores in the Gag-VLP coat, the effective n and dn/dT of the capsid layer will be 1.38-1.42 and $1.4\text{-}1.55\text{x}10^{-4}$ K^{-1}, respectively.

Fig. S1 shows that the temperature increase upon coat assembly is mainly observed within the VLP. Contributions to the PHI signal increase, are mainly coming from the AuNP core and the protein coat. The thermo-optical coefficients of AuNPs and protein correspond to $2.5\text{x}10^{-3}$ and 1.5 $\text{x}10^{-3}$ K^{-1} compared to $1\text{x}10^{-3}$ K^{-1} for water.[4] Considering the relative volumes of the protein layer and the core (2:1) and the average temperature increase in both layers, the overall contribution of the protein layer to the optical signal is ~20% of the signal increase upon VLP formation. This corresponds to about 4% of the total PHI signal in Gag-VLPs, which was considered negligible for the sake of simplifying the discussion.

Figure S1. Effect of the protein coat on the temperature profile for Au-Gag-VNPs at a heating laser power of 10uW. Displayed is the temperature profile as T(VNP)-T(AuNP) at various times along a sinusoidal heating pulse of 4us

duration. The inset shows the temperature change at the protein-water interface of VNPs. The main temperature increase occurs at the Au NP core. Within the protein layer of VLPs, the temperature profile exhibits a steep gradient that is observed due to differences in the heat capacity and thermal diffusivity of proteins and water. As a result of the slower thermal diffusion, a lower temperature is observed at the protein-water interface in VLPs as compared to the profile of AuNPs. The simulations have been conducted for the same amount of absorbed heat. Hence, the observed changes are due to the thermal properties of the respective layers. The maximum temperature increase is observed at the peak of the heating pulse. A larger dip at the protein-water interface is observed at longer times, which is consistent with the slower thermal diffusion in proteins compared to water.

Effect of refractive index change on the absorption cross section at the heating laser wavelength:
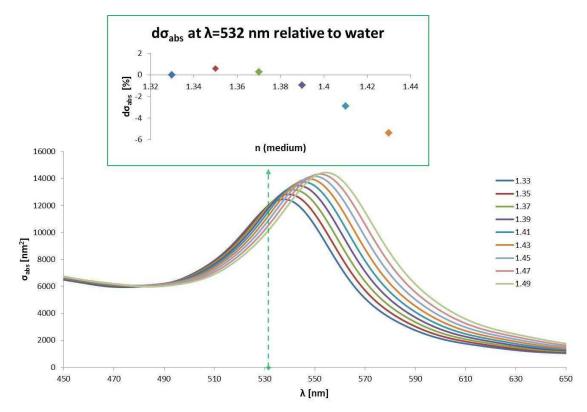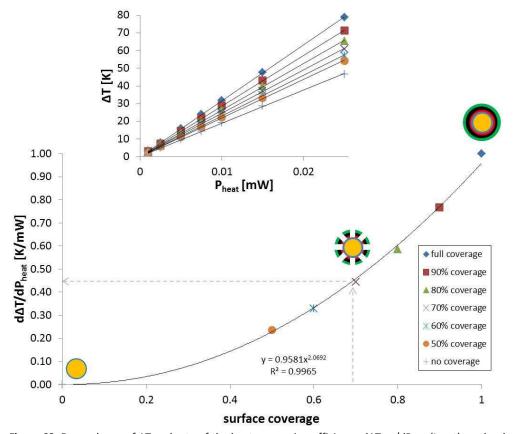

Figure S2. Shift in absorption cross section and peak position of plasmon resonance of a 60 nm AuNP with changes in the refractive index of the surrounding medium from n=1.33 to 1.49. The inset shows the change of the absorption cross section at the wavelength of the heating laser relative to the refractive index of water.

The plasmon frequency of Au NPs is sensitive to the index of refraction of the surrounding medium. Figure S2 shows the absorption spectra of a 60 nm Au NP embedded in a medium with a refractive index of n=1.33 to 1.49 calculated by finite-difference time-domain (FDTD) method. The dashed arrow indicates the wavelength of the heating laser used in PHI experiments. An increase in the refractive index of the medium results in a redshift of the plasmon peak and a change in the absorption cross section of the particles (Fig S2 inset).

Due to the compensation of both effects, the absorption cross section at the heating laser frequency observes a rather small change of ~5% for a 0.1 increase (1.33-1.43) in the refractive index. Moreover, as the field strength of the plasmon resonance falls off exponentially with distance from the nanoparticle surface, so does the sensitivity
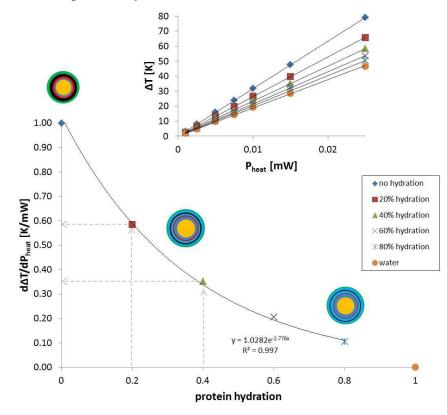
towards changes in the refractive index around the particle. In the case discussed here, the nanoparticle core is coated with a layer of DNA ~ 2 – 3 nm thick. Protein adsorption is likely to contribute a small amount of red-shift due to the PEG-DNA ligand layer that isolates the protein from the metal surface. In other words, the most sensitive region, near the surface of the AuNPs, stays unchanged upon assembly. Overall, we estimated the change in the absorption cross section at 532 nm at less than 2%, even for a complete protein shell.

Effect of surface coverage

Figure S3. Dependence of ΔT and rate of the heat conversion efficiency $d\Delta T_{max}/dP_{heat}$ (Inset) on the degree of surface coverage.

The maximum temperature of the Au NP core observed during a heating laser pulse was determined and plotted against the average heating laser power (Inset in Fig. S3). A linear increase of the core temperature with laser power was predicted. The slope of the linear regression ($d\Delta T/dP_{heat}$) represents the rate at which the sample converts absorbed heat into temperature change at different surface coverages. A plot of this heat conversion efficiency versus the protein coverage indicates a nonlinear dependence on the heating power with an exponent of ~2.1, Fig. S3.

Effect of protein hydration

Figure S4. Dependence of ΔT and the heat conversion efficiency $d\Delta T_{max}/dP_{heat}$ (Inset) on the degree of protein hydration.

To determine the rate of the drop in *ΔT* due to a change in hydration, the heat conversion efficiencies were plotted against the fractional hydration of the proteins and displayed in Figure S4. A negative exponential decay of the conversion efficiency was observed with increased protein hydration resulting in a diminution of *ΔT* by a factor of ~0.4 for a hydration of 20%. The densities, thermal conductivities and diffusivities of the hydrated protein layers were calculated assuming ideal protein-water mixtures. Heat conversion efficiencies were obtained for full surface coverage from the linear regression of the temperature rise against the laser heating power.

Table S1. Comparison of signal intensities obtained from distributions and heating intensity series of DNA-Au NPs and Gag-VNPs.

Sample	Mean$_{distr}$ [μV][a]	StDev$_{distr}$ [μV]	Responsivity [μV/μW]

DNA-AuNP	34.90	6.87 (19.7 %)	3.694
Gag-VNP	43.55	8.31 (19.1 %)	4.386

ª 10µW heating laser intensity

Overall, distribution analyses indicate a higher average signal increase of 24.8% as compared to the 18.7% for the heating series. The 6% deviation is likely sampling error due to the low number of particles recorded for the heating power series in Fig. 5 compared to the intensity distributions in Fig. 6.

References:

1.   Voros, J., The Density and Refractive Index of Adsorbing Protein Layers. *Biophys J* 2004, *87* (1), 553-61.
2.   Lin, L.-N.; Brandts, J. F.; Brandts, J. M.; Plotnikov, V., Determination of the Volumetric Properties of Proteins and Other Solutes Using Pressure Perturbation Calorimetry. *Analytical Biochemistry* 2002, *302* (1), 144-160.
3.   Nath, N.; Chilkoti, A., Label-Free Biosensing by Surface Plasmon Resonance of Nanoparticles on Glass: Optimization of Nanoparticle Size. *Analytical Chemistry* 2004, *76* (18), 5370-5378.
4.   Rashidi-Huyeh, M.; Palpant, B., Counterintuitive Thermo-Optical Response of Metal-Dielectric Nanocomposite Materials as a Result of Local Electromagnetic Field Enhancement. *Physical Review B: Condensed Matter and Materials Physics* 2006, *74* (7), 075405/1-075405/8.